TEM CHARACTERIZATION OF A FUSION ZONE IN P23/P91 WELDS

HOLEŠINSKÝ Jan[1], VODÁREK Vlastimil[2], VOLODARSKAJA Anastasia[2]

[1]*ArcelorMittal Ostrava a.s., Ostrava, Czech Republic, EU, jan.holesinsky@arcelormittal.com*
[2]*VSB - Technical University of Ostrava, Faculty of Metallurgy and Materials Engineering, Ostrava, Czech Republic, EU, vlastimil.vodarek@vsb.cz*

Abstract

Dissimilar welds are widely used in tubular systems of power plant boilers to compensate for different operating conditions. Redistribution of interstitial elements across the fusion line is regarded to be the most dangerous degradation mechanism in heterogeneous welds. Carbon and nitrogen move along the gradient of their chemical potential, in our case from P23 steel towards P91 steel. The paper deals with a TEM characterization of precipitation processes in fusion zones of two variants of heterogeneous P23/P91 welds after creep tests at 550 °C with times to rupture up to ca 80 000 hours. Both carbon extraction replicas and thin foils were studied. In carburized areas of welds heavy precipitation of carbides was observed, most of them corresponded to $M_{23}C_6$ carbides. The Cr/Fe ratio in these carbides continuously and systematically changed from the onset of carburized areas towards WM91 or P91 base material. This proved that carburization started in fusion zones, characterized by a continuous gradient of chemical composition. Furthermore, a low fraction of M_6X particles occurred in carburized areas. In adjacent partly decarburized areas of WM23 or P23 steel $M_{23}C_6$ and M_7C_3 particles dissolved during creep at 550°C. Furthermore, SAED investigations revealed precipitation of Laves phase of Fe_2W type in partly decarburized areas of both variants of P23/P91 welds. Precipitation of Laves phase has not been reported in P23 steel yet. Thermodynamic calculations proved that a reduction of carbon content in partly decarburized areas of WM23 or P23 steel made it possible to stabilize this minor phase.

Keywords: TEM, heterogeneous welds, fusion zone, minor phases

1. INTRODUCTION

Heterogeneous weldments are more frequently used in power plant blocks than homogeneous welds because they join components working in boiler systems at different conditions [1]. Usually low alloy and high alloy steels are welded. Creep resistance of such joints must reach at least creep strength of low alloy material. In heterogeneous welds a lot of attention is paid to weldability and welding technology, testing of their creep behaviour and microstructural evolution during long-term creep exposure [2].

Among root causes of heterogeneous weld degradation during high temperature service belong mismatch in physical properties and redistribution of interstitial elements due to gradients of chemical potentials of elements across the fusion zone. First of all, carbon redistribution is regarded as the most important degradation mechanism [3]. Atoms of carbon usually diffuse from the side of low Cr material into high Cr material. This diffusion process significantly affects microstructure evolution in close vicinity of fusion zone between low alloy and high alloy steel [1, 2]. Such decarburization during exposure at elevated temperature can cause progressive weakening in this area and it represents a very important mechanism of microstructural degradation of dissimilar welds. Decarburized zone in low alloy material is usually regarded as the critical region of heterogeneous welds during long-term creep exposure [4]. Detailed knowledge of the microstructure evolution in the fusion zone is therefore essential for understanding of the processes taking place during long-term creep exposure in dissimilar welds. The paper is aimed at transmission electron microscopy (TEM) characterization of precipitation processes in a fusion zone of P23/P91 dissimilar welds after long - term creep rupture tests at 550 °C, with times to rupture exceeding 80 000 hours.

2. EXPERIMENTAL MATERIALS AND PROCEDURES

2.1. Experimental materials

Welds A and B were made between P23 and P91 hot rolled steel pipes of the dimensions ø219 x 25 mm using a P91 matching filler metal (E CrMo 9 1B) in case of the Weld A and a P23 matching consumable (Thyssen Cr2WV) in case of the Weld B, respectively. The weld roots were fabricated by GTAW (141) technology followed by multi-pass welds (7 beads) formed by SMAW (111) process. The chemical compositions of base materials (BM) and weld metals (WM) are shown in **Table 1**. The post weld heat treatment (PWHT) regime of weldments was 750 °C / 2 hours / air. Uniaxial creep rupture tests were performed in air using cross-weld specimens (ϕ 6mm) at temperature of 550 °C at five stress levels in the interval from 150 to 100 MPa.

Table 1 Chemical compositions of base materials and weld metals, wt. %

Material	C	Mn	Si	Cu	Ni	Cr	Mo	V	Ti	Nb	W	N	Al
P23	0.08	0.55	0.27	0.04	0.08	2.11	0.07	0.23	0.06	0.01	1.70	0.013	0.012
WM23	0.07	0.44	0.20	0.04	0.17	2.47	0.06	0.25	0.01	0.02	1.62	0.018	N.A.
P91	0.11	0.51	0.38	0.17	0.42	8.67	1.00	0.23	0.01	0.07	0.01	0.048	0.012
WM91	0.11	0.66	0.21	0.04	0.82	9.50	1.02	0.22	0.01	0.04	0.06	0.028	N.A.

2.2. Sample preparation for TEM

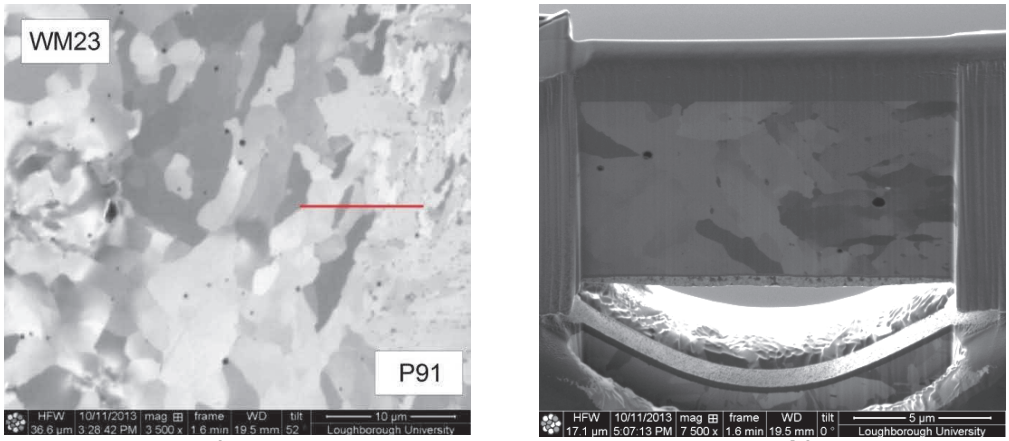

a) b)

Figure 1 Specimen B5 (t_r = 32 669hours) **(a)** SE image with the area of interest (fusion zone) marked by red line, **(b)** finally thinned TEM lamellae

Minor phase identification in specimens of heterogeneous welds was mostly carried out using carbon extraction replicas. In the case of the specimen B5 (Weld B, t_r = 32 699hours) focused ion beam (FIB) technique was applied for the site specific preparation of thin foil (**Figure 1a, 1b**). The area of interest corresponded to the fusion zone between P91 and WM23. Preparation of thin foil was carried out using dual beam microscope FEI NUOVA 600 NANOLAB (electron and ion beams), where milling is done by gallium ions.

2.3. Methods of transmission electron microscopy

Studies were carried out on a transmission electron microscope JEOL JEM 2100, equipped with an EDS analyser JEOL JED-2300T. Investigations were performed using a combination of bright field and dark field images and images in STEM mode. Identification of minor phases was carried out using a combination of EDS and selected area diffraction (SAED). Interstitial elements were not taken into account during semi-quantitative

analyses of EDS spectra. Results of semi-quantitative analyses were always normalized to 100 %. Furthermore EDS mapping was performed.

3. RESULTS AND DISCUSSION

3.1. Carburized zone in P91/WM91

Kinetic modelling predicted intensive precipitation of $M_{23}C_6$ carbides in the carburized zone of P91 steel [5]. Experimental investigations proved this prediction, most particles in that area were identified as $M_{23}C_6$ carbides. Dimensions and shapes of $M_{23}C_6$ particles in this area were very variable. Chemical composition of precipitates continuously changed from the side of P23 steel towards WM91 [6]. **Table 2** shows changes of $M_{23}C_6$ composition in the carburized area of the specimen A5 (Weld A, t_r = 81 095hours). Particles close to the partly decarburized zone of P23 steel contained tungsten and molybdenum, while particles on the side of WM91 contained only molybdenum. The Cr / Fe ratio in carbide particles increased towards WM91. This proves that the carburized area coincides, at least partly, with the fusion zone of the weld.

Table 2 Chemical composition of $M_{23}C_6$ carbides in the carburized zone, specimen A5, wt. %, where FZ is fusion zone

Position in FZ	V	Cr	Mn	Fe	Ni	Mo	W
on the side of P23	1.2 ± 0.2	50.6 ± 3.1	2.6 ± 0.3	26.4 ± 3.8	N.A.	8.3 ± 1.1	10.9 ± 2.1
on the side of WM91	0.7 ± 0.1	65.9 ± 1.0	1.7 ± 0.2	15.2 ± 0.3	1.1 ± 0.1	14.7 ± 1.0	0.7 ± 0.1

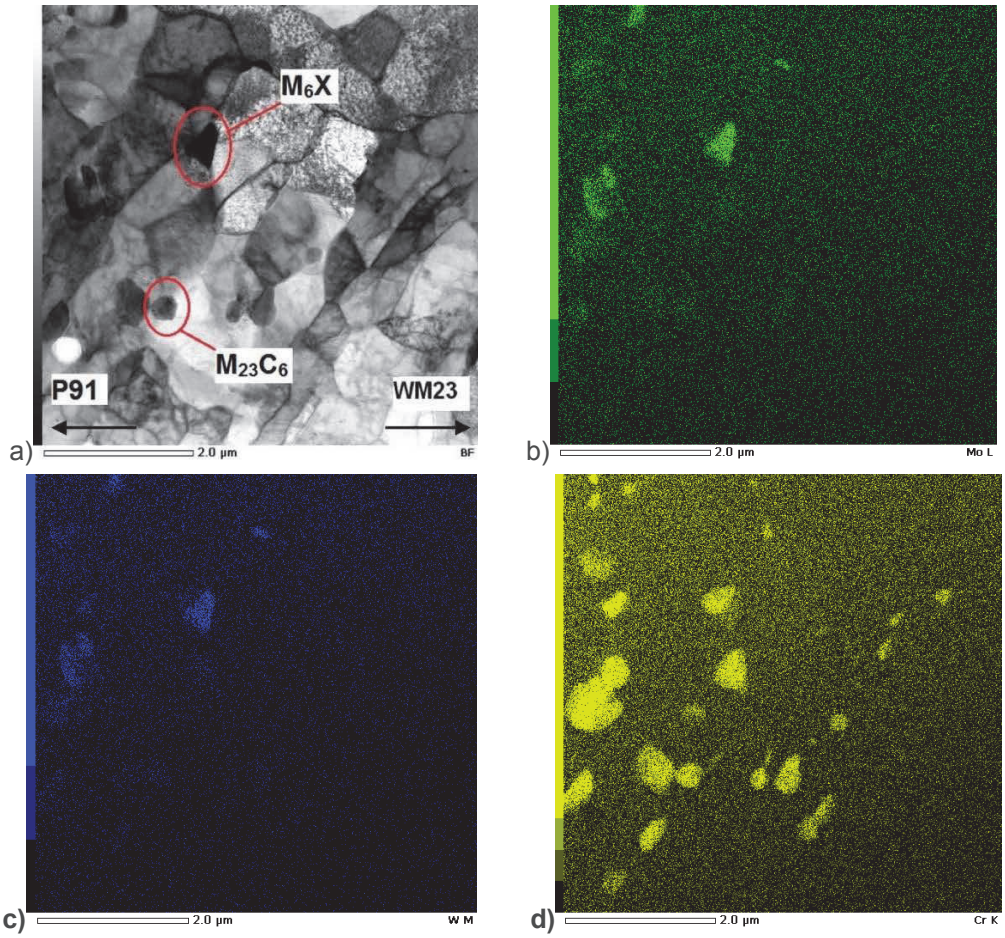

Figure 2 The beginning of the carburized zone in the fusion zone on the side of WM23 containing precipitates of M_6X a $M_{23}C_6$ phases **a)** bright field, **b)-d)** X - ray maps of Mo, W and Cr, respectively, sample B5

Furthermore, in the part of carburized area adjacent to the partly decarburized P23 steel a small number of coarse M_6X was identified. These carbonitrides could be stabilized by nitrogen redistributed together with carbon from P23 steel. **Figure 2a** shows the start of the carburized area in the thin foil prepared by FIB technique from the specimen B5 (Weld B). Chromium content in the matrix was evaluated as ca 2.5 wt. %. **Figures 2 b-d** represent X-ray maps of W, Mo and Cr, respectively. Areas rich in W and Mo correspond to a few M_6X particles. Areas rich in Cr are $M_{23}C_6$ particles. The occurrence of these two phases was confirmed by electron diffraction studies. In carburized areas of welds Laves phase particles were not identified.

3.2. Partly decarburized zone in P23 steel

Investigations on minor phases in the partly decarburized zone of P23 steel of the specimen A4 (Weld A, t_{rv}=v26 386hours) proved that during creep exposure at 550v°C total dissolution of M_7C_3 and $M_{23}C_6$ particles took place. Dissolution of M_7C_3 phase is in a good agreement with kinetic simulation for 550 °C / 30 000 hours. A reduced fraction of MX phase in this region also complies with this prediction [5]. Experimental studies proved that fine MX particles which did not dissolve in the partly decarburized zone of P23 steel were rich in Ti and W.

Investigations on precipitates in partly decarburized zones of specimens A4 and A5 revealed, except for fine MX particles, also coarse primary MX particles rich in Ti. Some of these particles reached the size of ca 200nm. Such particles were not identified in partly decarburized zone of WM23 in the Weld B, because there was no Ti present in the weld metal.

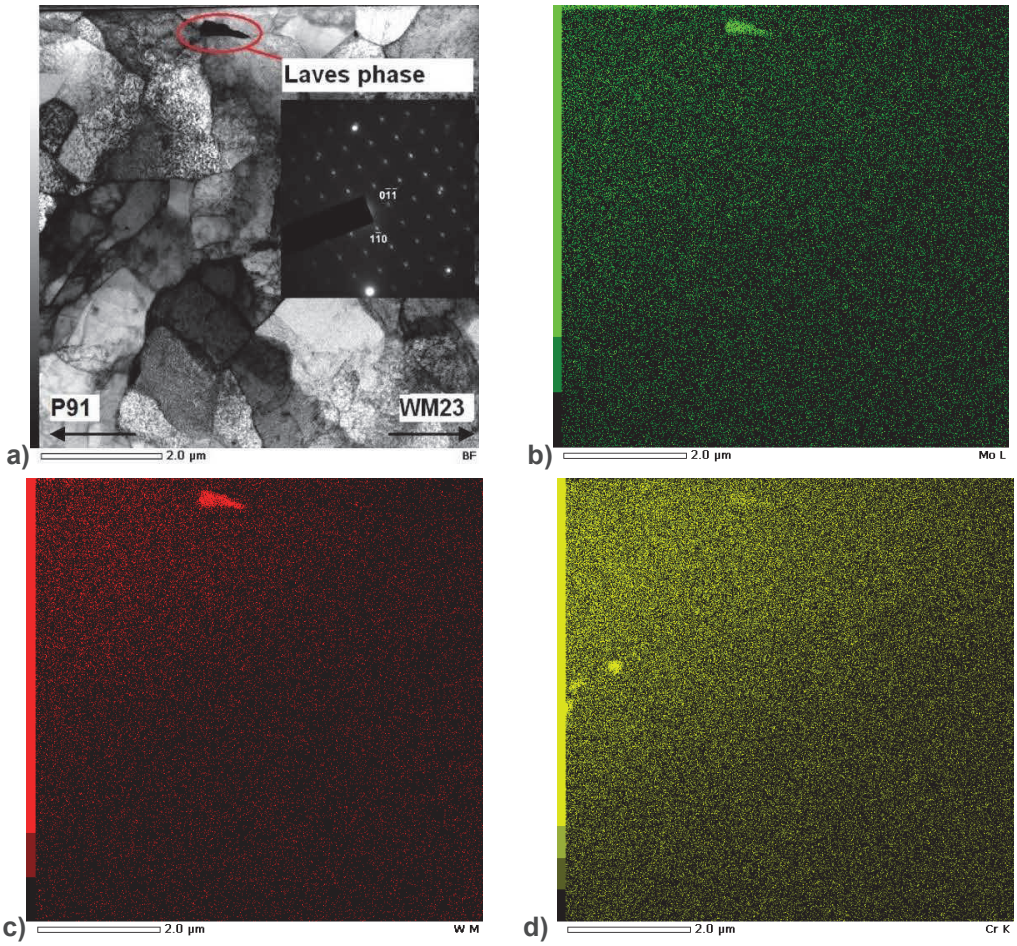

Figure 3 Partly decarburized zone of WM23,**a)** bright field (insert - diffraction pattern of Laves phase with zone axis $[11\bar{1}]_\eta$), **b)-d)** X-ray maps of Mo, W, Cr, respectively; specimen B5

Furthermore, coarse particles rich in W and Fe were also present in the partly decarburized zone of P23 steel. Their typical size was ca 200nm, but some particles were even coarser. Their chemical composition was close to composition of M_6X phase in P23 base material. Diffraction studies revealed two minor phases: M_6X and Laves phase of Fe_2W type. Reliable discrimination between these two minor phases based only on EDS results was not possible.

Internal defects in Laves phase resulted in diffusional "streaking" in spot diffraction patterns, **Figure 3a**. Unlike of M_6X phase precipitation of hexagonal Laves phase in steel P23 (WM23) was observed only in partly decarburized areas close to the fusion zone of heterogeneous welds, **Figure 3.** Precipitation of M_6X phase in P23 steel was identified by a number of authors [7, 8]. However, to the best knowledge of the authors, precipitation of Laves phase of Fe_2W type in P23 steel has not been reported yet.

Precipitation of Laves phase in the partly decarburized area of P23 (WM23) can be explained using thermodynamic modelling outputs. As per that Laves phase is predicted to be equilibrium phase in P23 steel containing less than ca 0.03 wt. % of carbon at temperature of 550 °C [5].

4. CONCLUSION

Most particles in carburized areas of P23/P91 welds were identified as $M_{23}C_6$ carbides. Chemical composition of precipitates continuously changed from the side of P23 (WM23) steel towards WM 91 (P91). The Cr / Fe ratio in carbide particles increased towards WM91 (P91) and also W was systematically replaced by Mo. This proves that carburized area coincides, at least partly, with the fusion zone of the weld. Furthermore, a low fraction of coarse M_6X particles was identified in the carburized area of P91 (WM91) adjacent to the partly decarburized zone. No Laves phase particles were identified in the carburized area of P91 (WM91).

Partial decarburization of P23 (WM23) steel in the course of creep exposure at 550 °C was accompanied by dissolution of M_7C_3 and $M_{23}C_6$ particles. Furthermore, decarburization of P23 steel resulted in precipitation of Laves phase (Fe_2W). Laves phase particles precipitated together with M_6X in the partly decarburized zone of P23 (WM23) and the chemical composition of both phases was similar, so the discrimination between these phases was possible only by combination of EDS and SAED. As per our best knowledge precipitation of Laves phase in P23 (WM23) steel has not been published yet. Observation of Laves phase in the partly decarburized zone of P23 (WM23) steel can be explained using thermodynamic modeling where the reduction of carbon content to level of ca 0.03 wt. % leads to its stability at 550 °C.

ACKNOWLEDGEMENTS

The authors wish to acknowledge the financial support from the projects No. LO1203 "Regional Materials and Technology Centre - Feasibility Programme", SP2017/60 and SP2017/58.

REFERENCES

[1] DAWSON, K. E. *Dissimilar Metal Welds*, Ph.D. thesis, Liverpool, 2012.

[2] STŘÍLKOVÁ,L., Creepové vlastnosti a struktura heterogenních svarů pro energetiku, Ph.D. thesis, Ostrava, 2013.

[3] HEUSER, H.,JOCHUM, C., BENDICK, W., HAHN, B., FUCHS, R. Welding of Dissimilar Joints of New Power Plant Steels. In *Proc. of Advances in materials technology for fossil power plants*, Florida, 2007.

[4] BARNARD, P.M., BUCHANAN, L.W., BARRIE, M. Material Development for Supercritical Boiler Pipeworks, In *Materials for Advanced Power Engineering 2010.* Jűlich: J. Lecomte - Beckers, 2010, pp. 39 - 54.

[5] ZLÁMAL B., FORET R., SOPOUŠEK J. Modelling of Phase Compositions of P23 and P91 Steels and their Welds", Technical Report, VUT Brno, 2007, pp. 1 - 28 (in Czech).

[6] HOLEŠINSKÝ, J., VODÁREK, V., SOJKA, J., STŘÍLKOVÁ L., KUBOŇ Z., SOZAŃSKA, M. Microstructural Stability of P23/P91 Dissimilar Welds during Creep at 550 °C. In *ECCC-Creep and Fracture Conference 2014*, Roma: CSM, 2014, CD ROM.

[7] HAKL, J, VLASÁK, T., BRZIAK, P., ZIFČÁK, P., *Žárupevné vlastnosti nízkolegované oceli 2.25%Cr-1.6%W-0.25%V*,Konference: Metal 2006, Hradec nad Moravicí, 2006, CD ROM.

[8] KUCHAŘOVÁ, K., SKLENIČKA, V., KVAPILOVÁ, M., SVOBODA, M. Creep and microstructural processes in a low-alloy 2.25%Cr1.6%W steel (ASTM Grade 23). *Materials Characterization*, 2015, vol. 109, pp. 1-8.